# Open quantum systems approach to atomtronics

R. A. Pepino, J. Cooper, D. Meiser, D. Z. Anderson, and M. J. Holland

*JILA, National Institute of Standards and Technology and Department of Physics, The University of Colorado,
Boulder, Colorado 80309-0440, USA*

We derive a quantum master equation to treat quantum systems interacting with multiple reservoirs. The formalism is used to investigate the atomic transport of bosons across a variety of lattice configurations. We demonstrate how the behavior of an electronic diode, a field-effect transistor, and a bipolar junction transistor can be realized with neutral, ultracold atoms trapped in optical lattices. An analysis of the current fluctuations is provided for the case of the atomtronic diode. Finally, we show that it is possible to demonstrate AND logic gate behavior in an optical lattice.

## I. INTRODUCTION

The emerging field of atomtronics [1–3] aims to construct analogies of electronic components, systems, and devices using ultracold atoms. In atomtronics, ultracold atoms move in an optical or magnetic potential in direct analogy with electrons moving in a semiconductor crystal. The motivation to construct and study atomtronic analogs of electronic systems comes from several directions.

First, the experimental atomtronic realizations promise to be extremely clean. Imperfections such as lattice defects or phonons can be completely eliminated. This allows one to study an idealized system from which all inessential complications have been stripped. Interest in such complixity-reduced systems lies parallel to the recent research efforts in single-electron transistors in mesoscopic systems [4] and molecules [5], where many themes common with atomtronics emerge. A consequence of the near-ideal experimental conditions for optical lattice systems is that theoretical descriptions for atomtronic systems can be developed from first principles. This allows theorists to develop detailed models that can reliably predict the properties of devices.

Second, atomtronics systems are richer than their electronic counterparts because atoms possess more internal degrees of freedom than electrons. Atoms can be either bosons or fermions, and the interactions between atoms can be widely varied from short to long range and from strong to weak. This can lead to behavior that is qualitatively different from that of electronics [6–9]. Consequently, one can study repulsive, attractive, or even noninteracting atoms in the same experimental setup. Additionally, current experimental techniques allow the detection of atoms with fast, state-resolved, near-unit quantum efficiency [10]. Thus it is possible, in principle, to follow the dynamics of an atomtronic system in real time.

Third, neutral atoms in optical lattices can be well isolated from the environment, reducing decoherence. They combine a powerful means of state readout and preparation with methods for entangling atoms [11]. Such systems have all the necessary ingredients to be the building blocks of quantum signal processors. The close analogies with electronic devices can serve as a guide in the search for new quantum information architectures, including novel types of quantum logic gates that are closely tied with the conventional architecture in electronic computers.

Fourth and finally, recent experiments studying transport properties of ultracold atoms in optical lattices [12–14] can be discussed in the context of the atomtronics framework. In particular, one can model the short-time transport properties of an optical lattice with the open quantum system formalism discussed here.

In this paper, we present a derivation of the master equation used to treat these specific open quantum systems. Afterward, we provide a detailed analysis of atomtronic analogies of the most elementary electronic components. These include conducting wires, diodes, and transistors. This work builds on a previous paper [3], providing a comprehensive explanation of the underlying analytical and numerical methods, and additional analysis of the components. Finally, we suggest how AND logic gate behavior can be recovered in this open-quantum-system setting.

This paper is organized as follows. In Sec. II we discuss the general master equation formalism, introducing the specific systems to be investigated, the defining properties of the reservoir, and the appropriate approximations necessary to complete the derivation for the models. In Secs. III and IV we apply the derived model to a variety of one-dimensional optical lattice systems in different open quantum system settings. The result is a collection of atomtronic devices that emulate electronic components.

## II. MODEL

### A. System

Unlike the typical behavior of their electronic counterparts, atomtronic devices operate at the few-particle level. The necessary repulsive correlations between particles are generally caused by either strong interactions for bosons or quantum statistical effects due to the Pauli exclusion principle for fermions. In this paper, we focus on bosonic current carriers, partly to draw the contrast with the electronic case.

The optical lattice provides a clean, controllable environment for atomtronics components. Strong atom-atom interactions can be precisely tuned if the atoms are confined in a tight optical lattice. Holding the atoms in a lattice has two primary advantages. First, the strength of the interactions is enhanced due to the confinement within the lattice wells and, second, by cooling of the atoms deep into the lowest Bloch

band regime, the center-of-mass motion of the atoms can be reduced to hopping between neighboring lattice sites. This results in a simple theoretical description as well as a clean experimental realization.

The dynamics of these ultracold atoms in this regime are accurately described by the Bose-Hubbard model [15,16]. In the lowest Bloch band, the Bose-Hubbard Hamiltonian is

$$\hat{H}_{\mathrm{BH}} = \sum_{i=1}^{N} \left( \epsilon_i \hat{N}_i + \frac{1}{2} U_i \hat{N}_i (\hat{N}_i - 1) \right) + \sum_{\langle i,j \rangle} (J_{ij} \hat{a}_i^\dagger \hat{a}_j + \mathrm{H.c.}), \tag{1}$$

where $i$ and $j$ are lattice site indices, $N$ is the total number of lattice sites, $\epsilon_i$ is the site energy, $U_i$ is the on-site interaction energy, $J_{ij}$ is the hopping energy, the sum $\langle i,j \rangle$ is taken between adjacent lattice sites, and $\hat{N}_i = \hat{a}_i^\dagger \hat{a}_i$. Here, $\hat{a}_i^\dagger$ and $\hat{a}_i$ are bosonic creation and annihilation operators, respectively, for an atom in the lowest Wannier orbital centered at site $i$. The precise tunability of the experimental parameters $\epsilon_i$, $U_i$, and $J_{ij}$ in the laboratory today make the realization of the custom lattices discussed in this work possible.

### B. Reservoir

The reservoirs serve two purposes in atomtronics: they are "sources" and "sinks" of particles. The reservoirs themselves could be experimentally realized in a variety of different ways. For instance, a reservoir source of atoms could be a one-dimensional optical lattice (Fig. 1), or a strongly-interacting 1-dimensional, harmonically trapped ultracold gas. Both of these systems have a desired Fermi sea-like energetic distribution that is discussed below. A reservoir sink of atoms could be a coupling of the system to vacuum modes of atoms in an untrapped state or the densely spaced modes of a nearly empty potential well. For modeling purposes, suitable reservoirs must meet several requirements. The system-reservoir correlations must decorrelate from the system faster than the time scale over which the state of the system changes appreciably. This allows
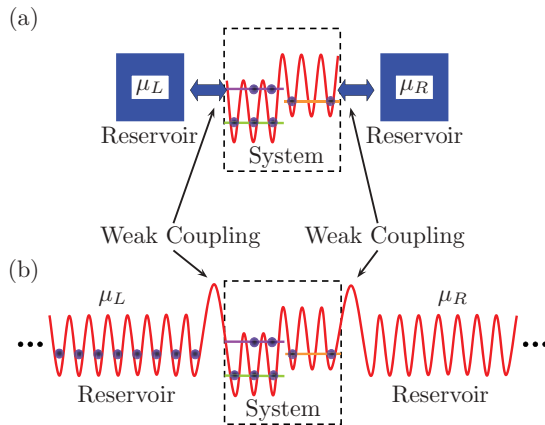


FIG. 1. (Color online) Illustration of an optical lattice, energetically tailored to have the transport response of an electronic diode, connected to two reservoirs whose respective chemical potentials induce an atomic transport from left to right.

one to make the Markov approximation. We will also assume that system and reservoirs are weakly coupled so that we can make the second-order Born approximation. Additionally, we assume that the density of states varies slowly over the spectrum of the system.

In the model used in this work, it is assumed that the reservoirs are strongly interacting bosons and, at low temperatures, the states in the reservoir are filled to the chemical potential, and all states above the chemical potential are empty. This is analogous to the situation in a semiconductor crystal, where to a good approximation the electrons occupy all states up to the Fermi energy. Labeling the single-particle excitations of the reservoir by a quantum number $k$, we can write the Hamiltonian of the reservoir as

$$\hat{H}_R = \sum_k \varepsilon_k \hat{R}_k^\dagger \hat{R}_k, \tag{2}$$

where $\varepsilon_k$ and $\hat{R}_k^\dagger$ are the energy and creation operator for the $k$th reservoir mode, respectively.

Such a reservoir can be constructed out of bosons trapped in a deep optical lattice potential. If the interactions between the atoms are very strong, and the temperature of the system is much lower than the interaction strength, the system enters the Mott-insulator regime, and by adjusting the chemical potential one can achieve a situation where each lattice site is occupied by precisely one atom. The atoms in this system could then be coupled to the atomtronic device to furnish a source of particles, as depicted in Fig. 1. By tailoring of the distribution of the energies $\varepsilon_k$ in the reservoir, it is possible to achieve a situation reminiscent of the Fermi sea reservoir. We may then represent the reservoir by a collection of uncoupled harmonic oscillators.

### C. Elimination of the reservoir: Master equation formulation

The quantum master equation approach is often used in quantum optics for describing open quantum systems [17–20]. In essence, it allows one to calculate observables associated with the evolution of a closed system without having to account for the free evolution of the reservoir. In this section we provide a detailed derivation of the master equation formulation for the system and reservoir described above. The derivation involves deriving an equation of motion for the reduced density operator for the system. Here we construct this equation of motion in a Liouville representation, since (as we discuss below) this form makes clear how one can go beyond the Born approximation, a necessity in this zero-temperature, unconventional setting.

The coupling of the system to the reservoir is by means of the exchange of particles between the system and the reservoir. The Hamiltonian for this interaction is

$$\hat{H}_V = \sum_{k,q} g_{kq} \hat{R}_k^\dagger \hat{a}_q + \mathrm{H.c.}, \tag{3}$$

where $\hat{a}_q$ is the annihilation operator for a particle in a system lattice site $q$ and $g_{kq}$ is the coupling matrix element between reservoir mode $k$ and site $q$.

The Hamiltonian for the system-reservoir interaction is given by

$$\hat{H} = \hat{H}_S + \hat{H}_R + \hat{H}_V, \tag{4}$$

where $\hat{H}_S = H_{\text{BH}}$ [Eq. (1)] in this work. For each part of the Hamiltonian we introduce an operation $\hat{\mathscr{L}}_x$, defined by its action on an arbitrary operator $\hat{\Theta}$ by

$$i\hat{\mathscr{L}}_x \hat{\Theta} = \frac{1}{i\hbar}[\hat{\Theta}, \hat{H}_x] \quad \text{where } x \in \{S, R, V\}. \quad (5)$$

We denote the density matrix of the system and reservoir with $\hat{\rho}$. From the full density matrix, the reduced density matrices $\hat{\sigma}_S$ and $\hat{\sigma}_R$ of system and reservoir are defined by tracing over the reservoir and system Hilbert spaces, respectively,

$$\hat{\sigma}_{S,R} = \text{Tr}_{R,S}[\hat{\rho}]. \quad (6)$$

We define the projection operator $\hat{\mathbb{P}}$ by

$$\hat{\mathbb{P}}\hat{\Theta} \equiv \hat{\sigma}_R \otimes \text{Tr}_R[\hat{\Theta}] \quad (7)$$

and its complement by $\hat{\mathbb{Q}} = \hat{\mathbb{1}} - \hat{\mathbb{P}}$. Under these definitions, $\hat{\mathbb{P}}$ and $\hat{\mathbb{Q}}$ satisfy the usual projection operator relationships $\hat{\mathbb{P}}^2 \hat{\Theta} = \hat{\mathbb{P}}\hat{\Theta}$, $\hat{\mathbb{Q}}^2 \hat{\Theta} = \hat{\mathbb{Q}}\hat{\Theta}$, and $\hat{\mathbb{P}}\hat{\mathbb{Q}}\hat{\Theta} = 0$. Using the projection operators, the reduced density matrix for the system can be written as

$$\hat{\sigma}_S = \text{Tr}_R[\hat{\mathbb{P}}\hat{\rho}]. \quad (8)$$

To find the equation of motion for $\hat{\sigma}_S$, we start from the evolution of the full density matrix $\hat{\rho}$:

$$\frac{d\hat{\rho}}{dt} = -i\hat{\mathscr{L}}\hat{\rho}, \quad (9)$$

where $\hat{\mathscr{L}} = \hat{\mathscr{L}}_S + \hat{\mathscr{L}}_R + \hat{\mathscr{L}}_V$. By noting that $\hat{\mathbb{P}} + \hat{\mathbb{Q}} = \hat{\mathbb{1}}$, this equation can be written as

$$\frac{d(\hat{\mathbb{P}} + \hat{\mathbb{Q}})\hat{\rho}}{dt} = -i(\hat{\mathbb{P}} + \hat{\mathbb{Q}})\hat{\mathscr{L}}(\hat{\mathbb{P}} + \hat{\mathbb{Q}})\hat{\rho}. \quad (10)$$

Acting with $\hat{\mathbb{P}}$ and $\hat{\mathbb{Q}}$ separates this equation into the coupled equations

$$\frac{d\hat{\mathbb{P}}\hat{\rho}}{dt} = -i[\hat{\mathbb{P}}\hat{\mathscr{L}}\hat{\mathbb{P}}\hat{\rho} + \hat{\mathbb{P}}\hat{\mathscr{L}}\hat{\mathbb{Q}}(\hat{\mathbb{Q}}\hat{\rho})], \quad (11)$$

$$\frac{d\hat{\mathbb{Q}}\hat{\rho}}{dt} = -i[\hat{\mathbb{Q}}\hat{\mathscr{L}}\hat{\mathbb{P}}\hat{\rho} + \hat{\mathbb{Q}}\hat{\mathscr{L}}\hat{\mathbb{Q}}(\hat{\mathbb{Q}}\hat{\rho})]. \quad (12)$$

The solution of Eq. (12) is

$$\hat{\mathbb{Q}}\hat{\rho} = -i\int_0^t e^{-i\hat{\mathbb{Q}}\hat{\mathscr{L}}\hat{\mathbb{Q}}\tau} \hat{\mathbb{Q}}\hat{\mathscr{L}}\hat{\mathbb{P}}\hat{\rho}(t-\tau)\,d\tau, \quad (13)$$

where we have assumed that the system and reservoir are initially uncorrelated, i.e., $\hat{\mathbb{Q}}\hat{\rho}(0) = 0$. Using this result to eliminate $\hat{\mathbb{Q}}\hat{\rho}$ in Eq. (11), we obtain

$$\frac{d\hat{\mathbb{P}}\hat{\rho}}{dt} = -i\hat{\mathbb{P}}\hat{\mathscr{L}}\hat{\mathbb{P}}\hat{\rho} - \hat{\mathbb{P}}\hat{\mathscr{L}}\hat{\mathbb{Q}}\int_0^t e^{-i\hat{\mathbb{Q}}\hat{\mathscr{L}}\hat{\mathbb{Q}}\tau}\hat{\mathbb{Q}}\hat{\mathscr{L}}\hat{\mathbb{P}}\hat{\rho}(t-\tau)\,d\tau. \quad (14)$$

Tracing over the reservoir Hilbert space leads to the equation of motion for the reduced density operator of the system,

$$\frac{d\hat{\sigma}_S(t)}{dt} = -i\hat{\mathscr{L}}_S\hat{\sigma}_S(t) + \int_0^t \mathscr{R}(\tau)\hat{\sigma}_S(t-\tau)\,d\tau, \quad (15)$$

where we have introduced the memory kernel

$$\mathscr{R}(\tau) = -\text{Tr}_R[\hat{\mathscr{L}}_V e^{-i(\hat{\mathscr{L}}_S + \hat{\mathscr{L}}_R + \hat{\mathbb{Q}}\hat{\mathscr{L}}_V\hat{\mathbb{Q}})\tau}\hat{\mathscr{L}}_V\hat{\sigma}_R]. \quad (16)$$

The first term on the right-hand side of Eq. (15) is the free system evolution while the second term describes the irreversible contribution due to the system-reservoir interaction.

Equation (15) is the exact master equation under the condition that the system and reservoirs are initially uncorrelated. All the dynamics due to the coupling to the reservoirs is encapsulated in $\mathscr{R}(\tau)$. Once the memory kernel is known, we can calculate the evolution of the reduced density matrix of the system without having to take into account the reservoirs explicitly. However, it turns out to be impossible to solve for the memory kernel exactly in even the simplest of circumstances, so approximations must be made to continue from this point.

Calculation of the memory kernel and its action on the system density matrix is straightforward under the Markov and Born approximations. The Markov approximation assumes that the correlation time $\tau_c$ between system and reservoir is much shorter than the time scales over which the reduced density matrix of the system changes appreciably, i.e.,

$$\tau_c \frac{d\hat{\sigma}_S}{dt} \ll \hat{\sigma}_S. \quad (17)$$

The Markov approximation consists of treating the system density matrix as a constant over time intervals of order $\tau_c$, and accordingly we can pull it out of the integral in Eq. (15). The short correlation time also allows us to extend the limit of integration in Eq. (15) to infinity.

The Born approximation takes the memory kernel to second order in $\hat{\mathscr{L}}_V$ and is thus a weak-coupling approximation. In the conventional Born approximation, $\hat{\mathscr{L}}_V$ is eliminated from the exponential term in the memory kernel. We cannot simply employ such an approximation here, however, since we are assuming that the strongly interacting boson gas obeys a zero-temperature Fermi-Dirac distribution characterized by $\mu_F$. The hard edge at the Fermi energy causes logarithmic divergences in the second-order energy shifts of system levels as $\mu_F$ approaches system resonances. This divergence occurs because, under the second-order approximation, as $\mu_F$ approaches a system resonance, the number of reservoir modes that the system is coupled to goes to 1—not a continuum of modes. This would induce Rabi flopping of the atom between the system and the reservoir and not the irreversible reservoir action intended. In reality, the interaction of the system with the reservoir taken to all orders mixes the modes and leads to decay, in this situation. Exact simulations on small systems show that we can recover the proper dynamics at the hard edge by including the influence of higher-order terms of the memory kernel expansion in $\hat{\mathscr{L}}_V$. We find that the fourth-order term in the expansion provides a good estimate for the higher-order corrections of the full memory kernel, yielding

$$\mathscr{R}(\tau) \approx -\text{Tr}_R[\hat{\mathscr{L}}_V\hat{\mathscr{L}}_V(-\tau)\hat{\sigma}_R e^{-[i(\hat{\mathscr{L}}_S + \hat{\mathscr{L}}_R)+\eta]\tau}], \quad (18)$$

where $\hat{\mathscr{L}}_V(\tau) = \exp[-i(\hat{\mathscr{L}}_S + \hat{\mathscr{L}}_R)\tau]\hat{\mathscr{L}}_V$. The evaluation of the fourth-order term shows that the decay $\eta$ is independent of $\mu_F$ unless $\mu_F$ approaches eigenenergies of the system. Even then, the dependence is small. Therefore, we take $\eta$ to be the mean value of the decay rate, which is where $\mu_F$ is equal to the system eigenenergy difference: $\eta = \mathscr{D}|g_q|^2\pi/(2\hbar^2)$, where $\mathscr{D}$ is the density of reservoir modes, assumed to be constant in the region of interest and $g_q$ is defined in Eq. (27). Introducing the rate at which particles enter or leave the system

$\Gamma_0 \equiv \mathscr{D}|g_q|^2/\hbar^2$, we have $\eta = \pi\Gamma_0/2$. It is reasonable to take this value for $\eta$ because $\eta$ is important only in the calculation for small deviations of $\mu_F$ about system resonances. The modified memory kernel in Eq. (18) captures the correct long-time behavior of the exact memory kernel.

With these approximations, the master equation becomes

$$\frac{d\hat{\sigma}_S}{dt} \approx -i\hat{\mathscr{L}}_S\hat{\sigma}_S - \int_0^\infty e^{-\eta\tau}\mathrm{Tr}_R[\hat{\mathscr{L}}_V\hat{\mathscr{L}}_V(-\tau)\hat{\sigma}_R]\,d\tau\,\hat{\sigma}_S(t).$$

(19)

Insertion of the Liouvillians into Eq. (19) yields

$$\frac{d\hat{\sigma}_S}{dt} \approx -i\hat{\mathscr{L}}_S\hat{\sigma}_S - \frac{1}{\hbar^2}\sum_k |g_{kq}|^2\int_0^\infty d\tau\,e^{-\eta\tau}$$

$$\times (\mathrm{Tr}_R\{[\hat{a}_q^\dagger\hat{R}_k,[\hat{a}_q(-\tau)\hat{R}_k^\dagger(-\tau),\hat{\sigma}_S\hat{\sigma}_R]]\}$$

$$+ \mathrm{Tr}_R\{[\hat{a}_q\hat{R}_k^\dagger,[\hat{a}_q^\dagger(-\tau)\hat{R}_k(-\tau),\hat{\sigma}_S\hat{\sigma}_R]]\}),$$

(20)

where we have used that

$$\mathrm{Tr}_R[\hat{\sigma}_R\hat{R}_k^\dagger\hat{R}_{k'}] = \delta_{k,k'}\langle\hat{R}_k^\dagger\hat{R}_k\rangle,$$

$$\mathrm{Tr}_R[\hat{\sigma}_R\hat{R}_k\hat{R}_{k'}^\dagger] = \delta_{k,k'}\langle\hat{R}_k\hat{R}_k^\dagger\rangle,$$

(21)

because the reservoir is in thermal equilibrium.

We project Eq. (20) onto the energy eigenbasis of the system and trace out the reservoir degrees of freedom. This allows us to evaluate the $\tau$ integral and to find a more explicit form of the master equation. Given two arbitrary system energy eigenstates $|a\rangle$ and $|b\rangle$ and adopting the notation $\langle a|\hat{\Theta}|b\rangle = \langle\hat{\Theta}\rangle_{ab}$, we have

$$\langle a|\hat{\mathscr{L}}_S\hat{\sigma}_S|b\rangle = \omega_{ab}\langle\hat{\sigma}_S\rangle_{ab},$$

$$\langle a|\hat{a}^\dagger(-\tau)|b\rangle = \exp(-i\omega_{ab}\tau)\langle\hat{a}^\dagger\rangle_{ab}$$

(22)

with $\hbar\omega_{ab} = (E_a - E_b)$ being the difference between the eigenenergies of $|a\rangle$ and $|b\rangle$. Similarly,

$$\langle k|\hat{R}^\dagger(-\tau)|j\rangle = \exp(-i\omega_{kj}\tau)\langle\hat{R}^\dagger\rangle_{kj}$$

(23)

for the reservoir. Performing the integral over $\tau$ produces the following closed form of the master equation:

$$\frac{d\langle\hat{\sigma}_S\rangle_{ab}}{dt} = -i\omega_{ab}\langle\hat{\sigma}_S\rangle_{ab} - \frac{1}{2}\sum_{c,d}\{\langle\hat{a}_q^\dagger\rangle_{ac}[(\Gamma_-^{(\mathrm{out})})_{cd}\langle\hat{a}_q\rangle_{cd}]$$

$$\times \langle\hat{\sigma}_S\rangle_{db} - [(\Gamma_-^{(\mathrm{out})})_{ac}\langle\hat{a}_q\rangle_{ac}]\langle\hat{\sigma}_S\rangle_{cd}\langle\hat{a}_q^\dagger\rangle_{db}$$

$$+ \langle\hat{\sigma}_S\rangle_{ac}[(\Gamma_-^{(\mathrm{in})})_{cd}\langle\hat{a}_q\rangle_{cd}]\langle\hat{a}_q^\dagger\rangle_{db} - \langle\hat{a}_q^\dagger\rangle_{ac}\langle\hat{\sigma}_S\rangle_{cd}$$

$$\times [(\Gamma_-^{(\mathrm{in})})_{db}\langle\hat{a}_q\rangle_{db}] + \langle\hat{a}_q\rangle_{ac}[(\Gamma_+^{(\mathrm{in})})_{cd}\langle\hat{a}_q^\dagger\rangle_{cd}]\langle\hat{\sigma}_S\rangle_{db}$$

$$- [(\Gamma_+^{(\mathrm{in})})_{ac}\langle\hat{a}_q^\dagger\rangle_{ac}]\langle\hat{\sigma}_S\rangle_{cd}\langle\hat{a}_q\rangle_{db} + \langle\hat{\sigma}_S\rangle_{ac}$$

$$\times [(\Gamma_+^{(\mathrm{out})})_{cd}\langle\hat{a}_q^\dagger\rangle_{cd}]\langle\hat{a}_q\rangle_{db} - \langle\hat{a}_q\rangle_{ac}\langle\hat{\sigma}_S\rangle_{cd}$$

$$\times [(\Gamma_+^{(\mathrm{out})})_{db}\langle\hat{a}_q^\dagger\rangle_{db}]\},$$

(24)

where

$$(\Gamma_\pm^{(\mathrm{in})})_{ab} = \frac{2}{\hbar^2}\sum_k \frac{|g_{kq}|^2}{\eta + i(\pm\omega_k - \omega_{ab})}\langle\hat{R}_k^\dagger\hat{R}_k\rangle,$$

(25)

$$(\Gamma_\pm^{(\mathrm{out})})_{ab} = \frac{2}{\hbar^2}\sum_k \frac{|g_{kq}|^2}{\eta + i(\pm\omega_k - \omega_{ab})}\langle\hat{R}_k\hat{R}_k^\dagger\rangle.$$

(26)

Note that

$$\lim_{\eta\to 0}\frac{1}{\eta + i(\pm\omega_k - \omega_{ab})}$$

$$= -i\mathcal{P}\frac{1}{\pm\omega_k - \omega_{ab}} + \pi\delta(\pm\omega_k - \omega_{ab}),$$

where $\mathcal{P}$ indicates that integrals are to be interpreted in the Cauchy principal value sense. The real parts of the $\Gamma_\pm$ matrices then give decay rates that agree with the Fermi golden rule result, while the imaginary parts give rise to level shifts in analogy with the Lamb shift in the hydrogen spectrum.

### D. Reservoir model

The detailed physics of the reservoirs influences the evolution of the system through the coupling matrix elements $g_{kq}$, the occupation expectation values of the reservoir modes $\langle\hat{R}_k^\dagger\hat{R}_k\rangle$, and the density of states of the reservoir. The reservoir model used below assumes strongly interacting bosons with a zero-temperature, Fermi sea-like energetic distribution. Thus, $\langle\hat{R}_k^\dagger\hat{R}_k\rangle = 1$ for all modes below the chemical potential of the reservoir and $\langle\hat{R}_k^\dagger\hat{R}_k\rangle = 0$ for all modes above. The coupling of the reservoir modes to the system states is a slowly varying function of the mode energy. We model it by a constant coupling up to some high-energy cutoff $\omega_c$ in order to quench the ultraviolet divergence that would otherwise arise, taking the form

$$|g_{kq}|^2 = |g_q|^2\theta(\omega_c - \omega_k),$$

(27)

with $\theta(\nu)$ the Heaviside step function. The high-energy cutoff $\omega_c$ is much larger than any relevant frequency of the system, and it does not affect the system's dynamics.

### III. ATOMTRONICS APPLICATIONS

In order to analyze the response of specific optical lattice configurations connected to reservoirs with different chemical potentials, we consider the steady-state solution of Eq. (24) and then proceed to solve for the matrix elements $\langle\hat{\sigma}_S\rangle_{ab}$. Once $\langle\hat{\sigma}_S\rangle_{ab}$ is known, expectation values of atomic currents $\langle\hat{J}_q\rangle$ into (and out of) a system site $q$ can be calculated from the reservoir's influence on the system population rates. For the population of each state, $d\langle\hat{\sigma}_S\rangle_{aa}/dt$, we sum up net rates out of the system state $|a\rangle$ and then subtract the net rates into the state. We then sum over all of the system states $|a\rangle$ to obtain the net current transport on system site $q$:

$$\langle\hat{J}_q\rangle = \sum_a\sum_{c,d}\{\langle\hat{a}_q^\dagger\rangle_{ac}[(\Gamma_-^{(\mathrm{out})})_{cd}\langle\hat{a}_q\rangle_{cd}]\langle\hat{\sigma}_S\rangle_{da}$$

$$+ \langle\hat{\sigma}_S\rangle_{ac}[(\Gamma_+^{(\mathrm{out})})_{cd}\langle\hat{a}_q^\dagger\rangle_{cd}]\langle\hat{a}_q\rangle_{da} - \langle\hat{a}_q^\dagger\rangle_{ac}\langle\hat{\sigma}_S\rangle_{cd}$$

$$\times [(\Gamma_-^{(\mathrm{in})})_{da}\langle\hat{a}_q\rangle_{da}] - [(\Gamma_+^{(\mathrm{in})})_{ac}\langle\hat{a}_q^\dagger\rangle_{ac}]\langle\hat{\sigma}_S\rangle_{cd}\langle\hat{a}_q\rangle_{da}\}$$

(28)

$$= \sum_a\sum_d\langle\hat{J}\rangle_{ad}\langle\hat{\sigma}_S\rangle_{da}$$

(29)

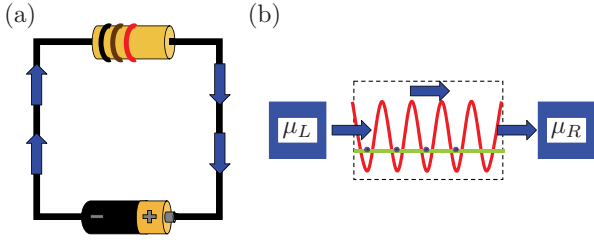$$= \mathrm{Tr}_S[\hat{J}_q\hat{\sigma}_S],$$

(30)

FIG. 2. (Color online) Illustration of the analogy between (a) the electronic circuit of a wire (with some inherent resistance) connected to a battery and (b) its atomtronic counterpart.

where

$$\langle \hat{J}_q \rangle_{ad}$$
$$= \sum_c \{ \langle \hat{a}_q^\dagger \rangle_{ac} [(\Gamma_-^{(out)})_{cd} \langle \hat{a}_q \rangle_{cd}] + [(\Gamma_+^{(out)})_{ac} \langle \hat{a}_q^\dagger \rangle_{ac}] \langle \hat{a}_q \rangle_{cd}$$
$$- [(\Gamma_-^{(in)})_{ac} \langle \hat{a}_q \rangle_{ac}] \langle \hat{a}_q^\dagger \rangle_{cd} - \langle \hat{a}_q \rangle_{ac} [(\Gamma_+^{(in)})_{cd} \langle \hat{a}_q^\dagger \rangle_{cd}] \} \quad (31)$$

is the current operator for site $q$ projected onto the system eigenbasis. Using this convention, the sign of $\mathrm{Tr}_S[\hat{J}_q \hat{\sigma}_S]$ reveals whether the current flows into ($-$) or out of ($+$) the system.

### A. Atomtronics analogy of a simple circuit

Here we analyze the atomtronics counterpart to a simple circuit of a battery connected to a resistive wire. As seen in Fig. 2, the analogy of a wire is an energetically flat optical lattice, with uniform tunneling rates and interaction energies ($\epsilon_j \equiv \epsilon$, $U_j \equiv U$, and $J_{ij} \equiv J$ for all neighboring sites). For this system, which is very weakly coupled to the reservoirs, we calculate the atomic current as a function of chemical potential difference. This numerical experiment is carried out by initially setting both left and right chemical potentials ($\mu_L$ and $\mu_R$) to zero. We raise $\mu_L$ so that an atomic transport is induced across the system from left to right and calculate the current out of the right side of the system $\langle J_R \rangle$ as a function of $\mu_L$. As shown in Fig. 3, the current increases with the chemical potential difference, but in quantized jumps that correspond directly to the left chemical potential overcoming the on-site interaction energy needed to introduce a greater number of atoms onto the left site. A closer examination of the numerical simulation implemented in Fig. 3 reveals two subtle features. As we move from left to right across the graph in Fig. 3, at the first current jump, occurring at $(\mu_L - \epsilon)/U = 0$, the current increases in two steps where one might expect to observe a single jump, since the condition to put a particle in the lattice is $\mu_L \geqslant \epsilon$. This is a result of the fact that the degeneracy of the Fock states in the one-particle manifold is split by $2J$ in the system state eigenbasis. In addition, the jump in current is broadened slightly by the nonzero $\eta$ and the system-reservoir coupling. This broadening, which makes the jump in current a smooth transition, is more apparent in the atomtronic devices presented below, where the system reservoir-coupling is taken to be orders of magnitude larger. Although the exact details for the second and third jumps are more complicated, the reasoning is the same: The eigenenergies are split by approximately $2J$,
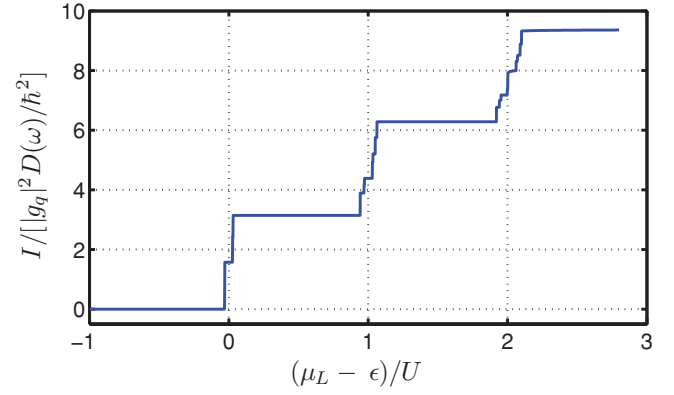


FIG. 3. (Color online) Current of the atomtronic wire, in the case of weak coupling to the reservoirs, as a function of the left chemical potential. The current monotonically increases in quantized jumps as the on-site interaction energy to put on an additional particle is overcome. The parameters used to model the atomtronic wire in this simulation are $\epsilon/U = 3$, $J/U = 3 \times 10^{-2}$, and $\hbar\Gamma_0/U = 10^{-6}$.

and the overall jump is smoothed out by $\eta$. These are general properties of all of the numerical experiments described in this work.

### B. The atomtronic diode

A diode is a device with an approximately unidirectional current characteristic. A voltage bias across the diode yields a current in one direction but not in the opposite direction if the voltage bias is reversed. Such behavior can be realized in an optical lattice by constructing an energy shift in half of an otherwise energetically flat lattice. We find that the diode characteristic persists as the number of lattice sites is increased. For simplicity, here we present the diode in a two-site lattice system. For the simulations in the rest of this paper, we assume $\epsilon/U = 3$, $J/U = 3 \times 10^{-2}$, and $\Gamma_0\hbar/U = 10^{-2}$.

In the Fock basis for a two-site system, there exist three states in the two-particle manifold: $|20\rangle$, $|11\rangle$, and $|02\rangle$, where $|nm\rangle$ refers to $n$ particles on the left site and $m$ particles on the right. The external energies of the two sites ($\epsilon_1$ and $\epsilon_2$) can be chosen so that the eigenstates $|20\rangle$ and $|11\rangle$ are approximately degenerate, leaving both states far detuned from $|02\rangle$. This configuration of the site energies is given by $\epsilon_1 = \epsilon$ and $\epsilon_2 = \epsilon_1 + U$. We refer to this as the "resonance condition."

Figure 4 illustrates how the resonance condition generates reverse-bias and forward-bias behavior in a two-site optical lattice. As seen in Fig. 4(a), if one holds the left reservoir chemical potential at $\mu_L = 0$ and raises the right reservoir chemical potential $\mu_R$, the system will undergo a transition from $|00\rangle$ to $|01\rangle$. The states $|01\rangle$ and $|10\rangle$ are separated in energy by $U$. As a result, most of the population remains in the $|01\rangle$ state. Increasing $\mu_R$ above the point where the transition from $|01\rangle$ to $|02\rangle$ is allowed causes the system to remain almost completely settled in the $|02\rangle$ state.

As seen in the Fig. 4(b), if one holds $\mu_R = 0$ and raises $\mu_L$, the system first undergoes a transition from $|00\rangle$ to $|10\rangle$. However, increasing $\mu_L$ so that the system evolves to $|20\rangle$ leads to a very different situation than in the above case: Since $|20\rangle$ is resonant with $|11\rangle$, both states are simultaneously populated.
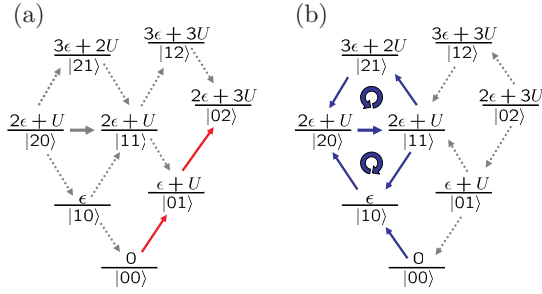
FIG. 4. (Color online) (a) Energy schematic of the reverse-bias dynamics of the two-site atomtronic diode. The red arrows represent the system transitions from an initially empty system. The gray (dotted) arrows represent all other possible transitions. Regardless of which state the system starts in, it evolves almost entirely to the $|02\rangle$ state. (b) Energy schematic of the forward-bias dynamics of the two-site atomtronic diode. Blue arrows illustrate transitions into current-bearing cycles, while gray (dotted) arrows represent all other possible transitions.

Since $\mu_R = 0$ takes all particles out of the site on the right, the system can make a transition from $|11\rangle$ back to $|10\rangle$. The combined effect of setting $\mu_L$ and $\mu_R$ to these values is to force the system to undergo a closed cycle of transitions between $|10\rangle$, $|20\rangle$, and $|11\rangle$. The result is a net atomic transport (or current flow) across the system. A second contributor to the net current through the system simultaneously arises since $\mu_L$ allows transitions from $|11\rangle$ to $|21\rangle$ as well. Thus, an additional current-generating cycle exists: $|11\rangle$ to $|21\rangle$ to $|20\rangle$ and back to $|11\rangle$. Both cycles contribute positively to a net current flow across the system.

For systems consisting of $N$ lattice sites, the diode configuration consists of two connected, energetically flat lattices whose energy separation is $\Delta\epsilon = U$. The dynamics do not change for larger systems since the degeneracy of the flat lattice allows for effective transport across the lattice; a particle allowed to enter the left site of half of the lattice is energetically degenerate with a particle found at the junction. Thus, there exist current cycles generated from the degeneracy between the $|222\cdots2\rangle \otimes |0\cdots000\rangle$ and $|222\cdots1\rangle \otimes |1\cdots000\rangle$ states. Going in the other direction, one can go to $|0\cdots000\rangle \otimes |222\cdots2\rangle$, but conditions are not energetically favorable to allow atomic transport across the junction. Figure 5 is a schematic of a four-site atomtronic diode in the forward-biased direction.

Supporting the claim that the diode remains qualitatively independent of the overall size of the lattice, Figs. 6(a) and
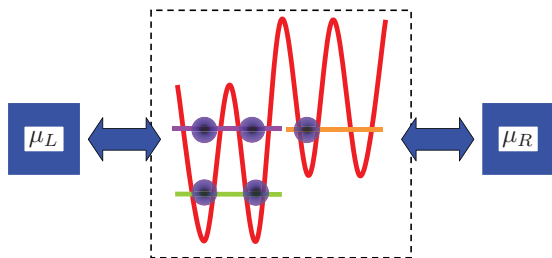


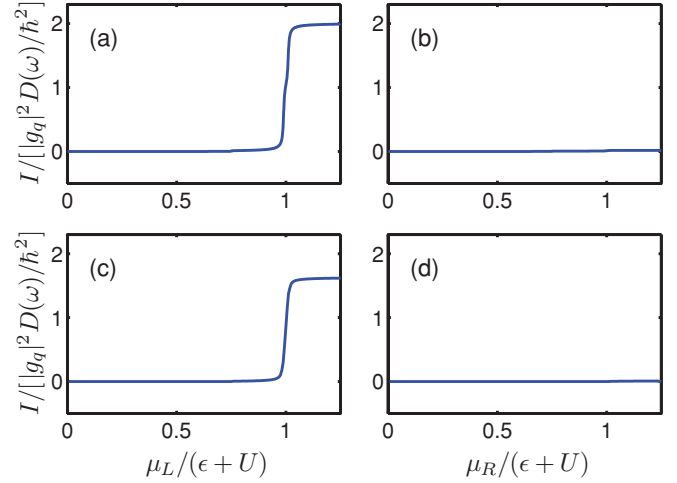FIG. 5. (Color online) Schematic of the four-site optical lattice atomtronic diode.



FIG. 6. (Color online) Current responses of (a) forward-bias two-site diode, (c) four-site diode as a function of $\mu_L$ (with $\mu_R = 0$), (b) reverse-bias two-site diode, and (d) four-site diode as a function of $\mu_R$ (with $\mu_L = 0$). The chemical potentials of all figures are normalized to the resonance condition, and the currents normalized to $\Gamma_0$.

6(b) and 6(c) and 6(d) are numerical simulations of the current responses of the two-site and four-site diodes, respectively. The general features of both diodes are qualitatively identical.

Given the current characteristics of the diode, one might ask how much the signal fluctuates. Recalling the current operator from Eq. (31), we can calculate the autocorrelation function for the current,

$$\langle \hat{J}_q(\tau + t)\hat{J}_q(t) \rangle = \text{Tr}_S[\hat{J}_q(\tau + t)\hat{J}_q(t)\hat{\sigma}_S], \quad (32)$$

using the quantum regression theorem.

To simulate an actual measurement, we convolve this correlation function with an exponentially decaying filter $\exp(-t/T)$. The Fourier transform of this convolution yields a time-averaged spectral density function $S(\omega, T)$. Our time-averaged signal-to-noise ratio $\mathcal{R}_{\text{SN}}$ as a function of $T$ is then

$$\mathcal{R}_{\text{SN}}(T) = \frac{\langle \hat{J}_q \rangle}{\sqrt{\int_0^\infty S(\omega, T)\, d\omega}}. \quad (33)$$

For long averaging times $T$ we find, for the conditions of Fig. 6,

$$\mathcal{R}_{\text{SN}}(T) \approx \sqrt{8\Gamma_0}\sqrt{T}. \quad (34)$$

For typical optical lattice experiments, $U \sim 1$ kHz is achievable, which implies that $\sqrt{8\Gamma_0} \sim 10\ \sqrt{\text{Hz}}$. Therefore, a signal-to-noise ratio of 10 can be achieved by averaging the atomic current for about 1 s.

### C. The atomtronic field-effect transistor

A field-effect transistor (FET) is a device that allows an externally applied field to affect the current through the device. This characteristic allows the FET to be utilized as an amplifier. Since the diode is optimized when the resonance condition is imposed on the optical lattice, small deviations from the resonance condition lead to large changes in maximum current propagating across the lattice. This is precisely the behavior
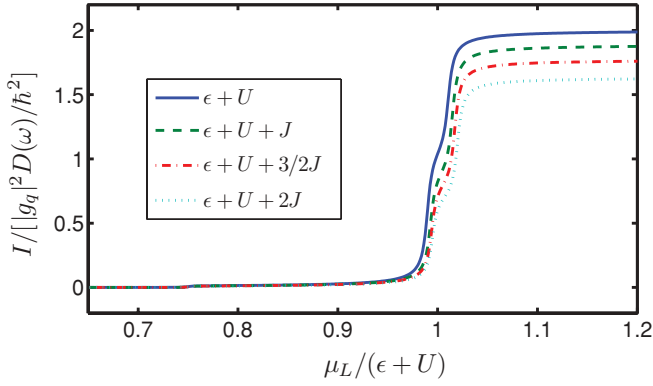
FIG. 7. (Color online) Current response of the atomtronic FET as a function of the chemical potential. Small changes in $\epsilon_2$ lead to appreciable changes in the current response. That is, as the system is detuned from its resonance condition, there is a falloff of the net current value across the device.

of a FET where a current is controlled by an applied voltage. In Fig. 7, we plot several current results for the forward-bias configuration as the separation in the external energy of the second site is raised past the resonance condition by fractions of $J$, the smallest system parameter in the model.

### D. The atomtronic bipolar junction transistor

A bipolar junction transistor (BJT) is a three-terminal device in which the overall current across the emitter and collector is controlled by a much weaker current via the base. Two practical applications of the BJT are signal amplification and switching (on and off) of the emitter current.

Realization of BJT-like behavior in atomtronic systems requires at least three sites connected to three different reservoirs. If the atomtronic diode is considered an atomtronic $p$-$n$ junction, one might guess that the atomtronic $n$-$p$-$n$ transistor would entail raising the external energy of the left and right (collector and emitter) sites higher than the middle (base) site by the on-site interaction energy. This configuration is illustrated in Fig. 8(a).

The degeneracy between the Fock states $|110\rangle$, $|020\rangle$, and $|011\rangle$ causes this configuration to yield BJT-like behavior.

We implement numerical simulations of this lattice configuration by fixing a chemical potential difference across the lattice. The left reservoir chemical potential $\mu_L$ is set to maintain one particle on the left site and the chemical potential of the right reservoir $\mu_R$ is set to zero. The middle chemical potential $\mu_M$ starts at zero and is increased to allow a single atom to enter the middle site.

When there are no atoms on the middle site, the configuration of the reservoirs pumps the system into the $|100\rangle$ Fock state [as seen in Fig. 8(b)]. The $|100\rangle$ and the $|001\rangle$ states are degenerate with each other, but the system must undergo a second-order, off-resonant transition via the $|010\rangle$ state from $|100\rangle$ to $|001\rangle$. Such transitions are suppressed by a factor of $(J/U)^2$ and thus become less likely as the energy difference between $|100\rangle$ and $|010\rangle$ increases. Thus, when the middle reservoir is set to maintain zero atoms on the middle site, the net current out of the emitter is minimal.
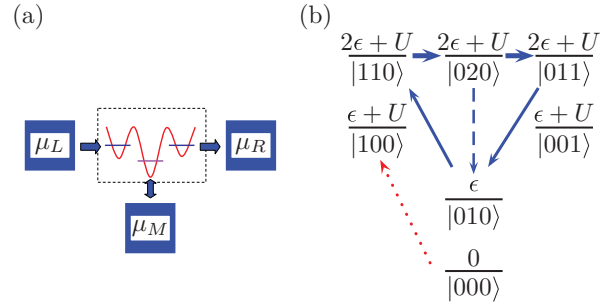


FIG. 8. (Color online) (a) Illustration of the BJT lattice-reservoir system. (b) The energy schematic of the three-site optical lattice under the extended resonance condition. Here the left reservoir is set to maintain an occupancy of one atom on the left site, and the right is set to remove all atoms. If the middle reservoir is set to remove all particles, then the system evolves to the $|100\rangle$ state (red dotted arrow). If the middle reservoir is set to maintain an occupancy of one atom on the middle site, then the degeneracy between states $|110\rangle$, $|020\rangle$, and $|011\rangle$ allows current to traverse the system.

When the middle reservoir's chemical potential is increased to allow a single atom into the middle site of the system, the degeneracy between the $|110\rangle$, $|020\rangle$, and $|011\rangle$ states is accessed, which allows atoms to travel across the system. One issue with this configuration is the following: in order to get to $|011\rangle$, the system has to make a transition through the $|020\rangle$ state. Since the middle reservoir is set to maintain an occupancy of one, but not two, atoms on the middle site, one of the atoms can be lost to the middle reservoir, leading to a loss of current out of the emitter. If the couplings of all three reservoirs to the system are equal, then the result is that the current measured passing through the base turns out to be even greater than the current measured out of the emitter. Thus, the system represents an inefficient transistor realization. On the other hand, if the middle reservoir were to be coupled weakly compared to the other reservoirs, then current would predominantly leave the system via the emitter, which is the desired behavior.

Figure 9(a) is a numerical simulation of the current out of the emitter and the base as a function of the base chemical potential. The coupling strength of the base connected to the reservoir is one-fifth the collector and emitter reservoir coupling. It should be noted that the region where the proposed
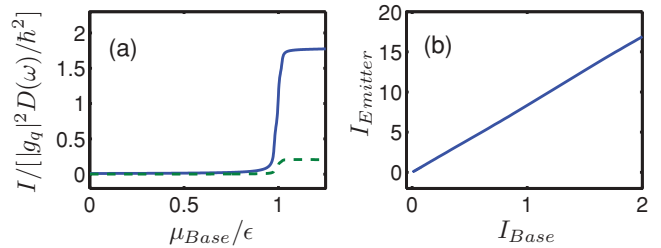


FIG. 9. (Color online) Characteristics of the atomtronic BJT. (a) For a fixed collector-emitter voltage bias, the current response measured through the base leg (green, dashed curve) and the emitter leg (blue curve) are plotted as a function of the base chemical potential. (b) The current out of the emitter is plotted vs the current out of the base. Here a large linear gain is observed.

TABLE I. AND gate truth table where the two inputs are labeled by $A$ and $B$, the output labeled by $O$, and the 1 or 0 entries represent on and off. (a) Truth table describing the device characteristics. (b) Numerical simulation of the atomtronic AND gate normalized to the maximal output current $O$. Here, the inputs $A$ and $B$ are the respective chemical potentials measured with respect to the on-site interaction energy ($\mu_A/U\ \mu_B/U$), and the output is the atomic current normalized by the maximum output current ($I/I_{max}$). In practice, the logical ins and 'outs are never really 0 or 1' but are defined by setting threshold values. Since the maximal output current is larger than all other output values by at least a factor of 6.25, we can conclude that there exists logic gate behavior in this optical lattice setup.

| (a) AND gate | | | (b) Atomtronic AND gate simulation | | |
|---|---|---|---|---|---|
| $A$ | $B$ | $O$ | $A$ | $B$ | $O$ |
| 0 | 0 | 0 | 0 | 0 | 0.00 |
| 1 | 0 | 0 | 3.2 | 0 | 0.01 |
| 0 | 1 | 0 | 0 | 3.2 | 0.16 |
| 1 | 1 | 1 | 3.2 | 3.2 | 1.00 |

atomtronic transistor mimics the electronic BJT is limited to the transition region, or current jump. One can increase the length of this region by increasing the overall system-reservoir coupling strength. Figure 9(b) shows that the gain of this device is fairly linear.

## IV. DISCRETE ATOMTRONICS LOGIC

Integrated circuits are designed with a very large number of transistor elements to perform a desired function. The demonstrated ability to realize atomtronic diodes and transistors thus motivates the question as to whether higher functionality can be realized with these ultracold atomic systems. Here we look at the most fundamental of these, the atomtronic AND logic gate.

A traditional logic element is a device with a given number of inputs and outputs, composed of switches, that generates a series of logical responses. Such logical behavior can be expressed in a truth table composed of 1's and 0's ("ons" and "offs"). Logic elements are the fundamental building blocks of computing and discrete electronics. In Table I(a) the truth table for the AND logic gate is given as an example. The next level of complexity in emulating electronic systems is to create logic elements from the atomtronic components.

An AND gate is a device with two inputs ($A$ and $B$) and one output ($O$). As illustrated in Table I(a), the device characteristic of the AND gate is that $O$ remains off unless both $A$ and $B$ are on. In electronics, such a device can be constructed by connecting two transistors in series [as illustrated in Fig. 10(a)]. By analogy, if the atomtronic BJTs are connected in the same series configuration [as illustrated in Fig. 10(b)], the AND gate truth table can be generated.

In the construction of practical logic circuits, the values of the 1's and 0's are not strict values, they are defined within a given range. The data in Table I(b) have been generated
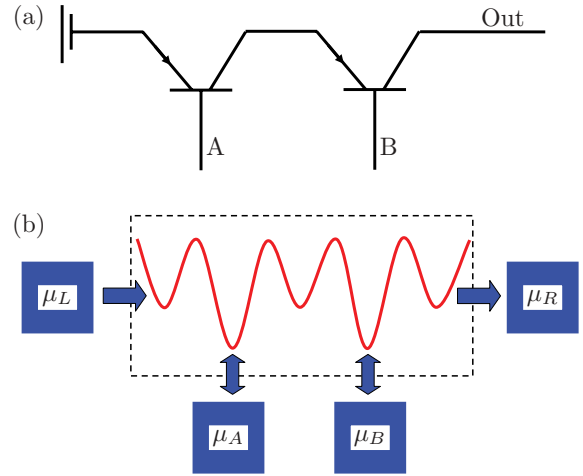


FIG. 10. (a) Electronic schematic for the AND logic gate, a device constructed by cascading two transistors in series. (b) Atomtronics and schematic. The atomtronic AND logic gate is constructed exactly like its electronic counterpart, i.e., by cascading two transistors in series. A chemical potential bias $\mu_L - \mu_R$ across the device attempts to drive a current across the device. No substantial current is observed, however, unless both $\mu_A$ and $\mu_B$ supply atoms onto the base terminals of their respective transistors.

in a numerical experiment of the configuration depicted in Fig. 10(b). For this particular experiment, the maximal current out of the device is at least a factor of 6.25 greater than any other measured current out. Thus a discernible difference between on and off is observed, and the output currents reproduce the AND gate truth table. Such a difference can also be enhanced by increasing the on-site interaction energy $U$ of the lattice.

## V. CONCLUSIONS

In this paper, we have derived a general model for treating a specific class of open quantum systems where the reservoirs act as sources and sinks for particles moving into and out of the system. Such a formalism can be used to study atomic transport across arbitrary multiple potential well configurations. Here, the formalism was used to show how neutral atoms in custom optical lattices can exhibit electronic diode, FET, BJT, and and gate behavior.

Looking forward, we aim to develop more complicated atomtronic devices such as additional logic elements, flip-flops, and constant current sources by cascading our current atomtronic components in a manner analogous to the development of more sophisticated electronic devices. The simulation of the AND gate is promising since it demonstrates the possibility of cascading atomtronic components to make more sophisticated devices.

[1] A. Micheli, A. J. Daley, D. Jaksch, and P. Zoller, Phys. Rev. Lett. **93**, 140408 (2004).

[2] J. A. Stickney, D. Z. Anderson, and A. A. Zozulya, Phys. Rev. A **75**, 013608 (2007).

[3] R. A. Pepino, J. Cooper, D. Z. Anderson, and M. J. Holland, Phys. Rev. Lett. **103**, 140405 (2009).

[4] D. M. Cardamone, C. A. Stafford, and S. Mazumdar, Nano Lett. **6**, 2422 (2006).

[5] C. A. Stafford, D. M. Cardamone, and S. Mazumdar, Nanotechnology **18**, 424014 (2007).

[6] M. Theis, G. Thalhammer, K. Winkler, M. Hellwig, G. Ruff, R. Grimm, and J. H. Denschlag, Phys. Rev. Lett. **93**, 123001 (2004).

[7] S. Inouye, M. R. Andrews, J. Stenger, H.-J. Miesner, D. M. Stamper-Kurn, and W. Ketterle, Nature (London) **392**, 151 (1998).

[8] S. Inouye, J. Goldwin, M. L. Olsen, C. Ticknor, J. L. Bohn, and D. S. Jin, Phys. Rev. Lett. **93**, 183201 (2004).

[9] C. A. Stan, M. W. Zwierlein, C. H. Schunck, S. M. F. Raupach, and W. Ketterle, Phys. Rev. Lett. **93**, 143001 (2004).

[10] W. Bakr, J. Gillen, A. Peng, S. Fölling, and M. Greiner, Nature (London) **462**, 74 (2009).

[11] O. Mandel, M. Greiner, A. Widera, T. Rom, T. W. Hänsch, and I. Bloch, Nature (London) **425**, 937 (2003).

[12] N. Strohmaier, Y. Takasu, K. Gunter, R. Jordens, M. Kohl, H. Moritz, and T. Esslinger, Phys. Rev. Lett. **99**, 220601 (2007).

[13] K. Henderson, H. Kelkar, B. Gutiérrez-Medina, T. C. Li, and M. G. Raizen, Phys. Rev. Lett. **96**, 150401 (2006).

[14] J. H. Denschlag, J. E. Simsarian, H. Haeffner, C. McKenzie, A. Browaeys, D. Cho, K. Helmerson, S. L. Rolston, and W. D. Phillips, J. Phys. B **35**, 3095 (2002).

[15] D. Jaksch, C. Bruder, J. I. Cirac, C. W. Gardiner, and P. Zoller, Phys. Rev. Lett. **81**, 3108 (1998).

[16] M. Greiner, O. Mandel, T. Esslinger, T. W. Hänsch, and I. Bloch, Nature (London) **415**, 39 (2002).

[17] C. Cohen-Tannoudji, J. Dupont-Roc, and G. Grynberg, *Atom-Photon Interactions*, Chap. 4 (Wiley, New York, 1992).

[18] P. Meystre and M. Sargent, *Elements of Quantum Optics*, 3rd ed., Chap. 15, Sec. 1 (Springer-Verlag, Berlin, 1999).

[19] D. F. Walls and G. J. Milburn, *Quantum Optics*, Chap. 6, Sec. 1 (Springer-Verlag, Berlin, 1994).

[20] D. N. Zubarev, V. Morozov, and G. Röpke, *Statistical Mechanics of Nonequilibrium Processes*, Vol. 2, Chap. 7 (Akademie-Verlag, Berlin, 1997).